Compensation mechanism in high purity semi-insulating 4*H*-SiC

W. C. Mitchel[a] and William D. Mitchell
Air Force Research Laboratory, AFRL/MLPS, Wright-Patterson AFB, Ohio 45433-7707

H. E. Smith, G. Landis, and S. R. Smith
University of Dayton Research Institute, 3000 College Park, Dayton, Ohio 45469

E. R. Glaser
Naval Research Laboratory, Washington, District of Columbia 20375

(Received 15 November 2006; accepted 19 December 2006; published online 15 March 2007)

A study of deep levels in high purity semi-insulating 4*H*-SiC has been made using temperature dependent Hall effect (TDH), thermal and optical admittance spectroscopies, and secondary ion mass spectrometry (SIMS). Thermal activation energies from TDH varied from a low of 0.55 eV to a high of 1.65 eV. All samples studied showed *n*-type conduction with the Fermi level in the upper half of the band gap. Fits of the TDH data to different charge balance equations and comparison of the fitting results with SIMS measurements indicated that the deep levels are acceptorlike even though they are in the upper half of the band gap. Carrier concentration measurements indicated that the deep levels are present in concentrations in the low 10^{15} cm^{-3} range, while SIMS results demonstrate nitrogen and boron concentrations in the low to mid-10^{15}-cm^{-3} range. The results suggest that compensation in this material is a complex process involving multiple deep levels.
© *2007 American Institute of Physics*. [DOI: 10.1063/1.2437677]

INTRODUCTION

Semi-insulating SiC substrates are widely used for growth of both SiC and nitride based electronic device structures. The semi-insulating properties can be created by compensating shallow donor and acceptor levels from residual impurities with intrinsic deep level defects. The report of such high purity semi-insulating (HPSI) SiC was made in 2000,[1] but the exact nature of the intrinsic defects involved and the compensation mechanisms in this material are still under investigation so the electronic levels due to intrinsic defects in HPSI SiC are of both technological and fundamental interest. The thermal activation energies of HPSI 4*H*-SiC measured by temperature dependent Hall effect (TDH) or resistivity measurements[2,3] have been reported to cover a broad range from 0.9 to 1.5 eV, suggesting that different defects or defect levels might be involved in the compensation mechanism. Indeed several intrinsic defects have been found in SiC using electron paramagnetic resonance (EPR) experiments but much of this work was done on radiation damaged material and not as-grown material. Early EPR measurements on unirradiated HPSI 4*H*-SiC detected carbon vacancies V_C.[4,5] Later the P6/P7 defects were detected in as-grown HPSI material,[6] and most recently a full spectrum of defects including V_{Si}, V_C-V_{Si}, and V_C-C_{Si} have been reported.[7] Energy levels for these defects have been estimated from the spectral response of the individual signals during photo-EPR experiments. Correlations between the photo-EPR energies and activation energies measured by temperature dependent resistivity measurements have been attempted.[8] However, reports of defect concentrations from EPR experiments are rare and while Son *et al.*[8] report defect concentration on the order of the boron and nitrogen concentrations, Zvanut *et al.*[9] reported much lower concentrations for V_C and Carlos *et al.*[10] reported that the only defect with concentrations high enough to affect the compensation was P6/P7.

The lack of any correlation between defect concentrations and deep level concentrations makes conclusions based on photo-EPR and resistivity measurements of activation less than conclusive. Deep level transient spectroscopy (DLTS) is capable of providing deep level concentrations and a number of defect related levels have been reported in both irradiated and as-grown SiC. However, this technique cannot be performed on semi-insulating samples and so all reports have been for doped material, either *n* or *p* type. Also, in most cases in SiC, DLTS requires assumptions about the temperature dependence of the capture cross section. This leads to slightly different E_a's for the same defect when measured and analyzed in different laboratories. A multiplicity of nomenclature also complicates matters. None the less, DLTS provides a valuable catalog of possible deep levels that may take part in the compensation of residual shallow level impurities. Dalibor *et al.*,[11] Lebedev,[12] and Hemmingsson *et al.*[13] provide summaries of the known deep levels produced by irradiation as of 1999. A more recent report is that of Storasta *et al.*[14] While there have been many reports since, including as-grown bulk and epitaxial materials, all intrinsic deep levels in the upper half of the band gap can be identified with one of the levels in these three reports, even if the notations used by various groups to name the deep levels is somewhat confusing. Table I summarizes the deep levels in the upper half of the band gap of 4*H*-SiC that are pertinent to this study of compensation in HPSI material. The notation is mixed but is consistent with most of the more recent literature. $Z_{1/2}$ and EH4 and RD_4 and EH6/EH7 have been listed separately because of the differences in capture cross sec-

[a]Electronic mail: william.mitchel@wpafb.af.mil

 © 2007 American Institute of Physics

Downloaded 14 Aug 2007 to 132.250.134.160. Redistribution subject to AIP license or copyright, see http://jap.aip.org/jap/copyright.jsp

TABLE I. Deep levels by DLTS reported in the literature in the upper half of the band gap of 4*H*-SiC. T is the temperature the trap is observed at, E_a is an average of the activation energies reported for the trap measured from the bottom of the conduction band, and σ is the best value for the capture cross section.

Trap	T (K)	E_a (eV)	σ (cm^{-2})	Ref.
EH1 (S_1)	180	0.45	5×10^{-15}	13 and 14
$Z_{1/2}$	310	0.67	5×10^{-14}	11
EH3 (S_2)	320	0.71	1×10^{-16}	14
$RD_{1/2}$	450	0.93	8×10^{-15}	11
EH5	560	1.03	1×10^{-16}	13
RD_4	660	1.49–1.60	5×10^{-14}	11
EH6/7	600	1.65	2×10^{-13}	13 and 14

tions, although reported E_a's for these levels overlap. $Z_{1/2}$,[11] EH6/7,[15,16] and $RD_{1/2}$ (Ref. 17) have been observed in unirradiated, as-grown epitaxial material. Most researchers report that the intrinsic deep levels observed by DLTS in the upper half of the band gap are acceptorlike.

The thermal stability of defects is important for maintaining semi-insulating properties during epitaxial growth and device processing. Most DLTS studies of intrinsic defects report annealing properties of the defects, but the results on irradiated material must be taken with care when comparing them with the thermal stability of as-grown HPSI material because irradiation produces copious amounts of simple defects, Frenkel pairs, in particular, and the presence of interstitials and vacancies can reduce the effective annealing temperature compared with grown-in defects. Zhang *et al.*, however, studied deep levels in as-grown material. They report that $Z_{1/2}$ is relatively stable after 1650 °C annealing but that EH6/7 has a more complex annealing behavior. They also report that the original peak disappears and another smaller one appears at a slightly lower temperature. They speculate that this center might be two defects, one of which anneals out and the other does not, or that one center anneals into a completely different one. Negoro *et al.* confirmed the relative stability of $Z_{1/2}$ at 1600 °C but saw only a slight reduction in EH6/7 concentration after 1600 °C but a large reduction after 1800 °C. They reported a slight increase in $RD_{1/2}$ after annealing.

Temperature dependent Hall effect is a valuable technique for the study of semi-insulating material because it gives the thermal activation energy of semi-insulating material under study, which can be different from the energies detected by photo-EPR and DLTS due to Frank-Condon-like shifts in energy due to defect configuration changes. Under the right circumstances, TDH can also give the concentration of the level, pinning the Fermi level and the concentration of the compensating centers. These concentrations can then be compared with concentrations from other, more defect specific, experiments such as EPR. However, very little has been reported on TDH measurements of semi-insulating SiC. Mitchel *et al.*[3] reported activation energies ranging from 0.9 to 1.5 eV with *n*-type conduction but the Hall data were not adequate for extracting deep level and compensation concentrations. We report here a more complete TDH study of a series of HPSI 4*H*-SiC samples in which the relevant concentrations could be extracted along with the activation energies. We also report thermal and optical admittance spectroscopy (TAS and OAS) experiments on selected samples. Compensating center concentrations from TDH are compared with secondary ion mass spectrometry (SIMS) results. A model of compensation is presented.

EXPERIMENTAL DETAILS

The HPSI 4*H*-SiC crystals in this study were grown at Cree, Inc. by the physical vapor transport (PVT) process. Most of the crystals were grown as part of research and development contracts and as such are research crystals that do not necessarily represent commercial quality material. Some of the research crystals had lower resistivities than would be considered acceptable for sale as semi-insulating material but enabled us to study the full range of deep levels in undoped material. Several commercial wafers from Cree, Inc. were included in the study as well for completeness. Growth conditions, such as the stoichiometry and growth temperature, were not reported but all samples were grown using high purity source material without intentional doping. Individual wafers were supplied and van der Pauw square samples were cut from them. Sample size varied from about 8×8 mm^2 to 6×6 mm^2. Prior to contacting, the samples were oxidized at 1150 °C for several hours followed by a HF etch to remove polishing damage. Ohmic contracts were formed by alloying Ta/NiCr/W at 925 °C for 2 min in forming gas followed by deposition of Cr/Au contact pads. TAS and OAS samples had InSnO Schottky contacts. TDH measurements were made in a guarded, high impedance system in flowing nitrogen ambient. Annealing studies separate from the contacting procedures were made in a resistance heated furnace in an argon ambient. The samples were sandwiched between sacrificial SiC wafers and were oxidized and etched after annealing and before contacts were redeposited.

Thermal activation energies were determined from resistivity or carrier concentration versus temperature data by one of several analysis techniques. For samples where the carrier concentration or resistivity versus inverse temperature data lacked curvature, the activation energy was determined by fitting that data to[18]

$$\log(n \text{ or } \rho^{-1})T^{-1.5} = Ae^{-E_a/kT}, \tag{1}$$

where n is the carrier concentration and ρ is the resistivity. The $T^{-1.5}$ term takes into account the temperature dependence of the density of states. It should be noted that when ρ is used in Eq. (1) the temperature dependence of the mobility will affect the calculated activation energy. When the scatter in the carrier concentration data was low enough and the n vs $1/T$ data showed curvature, the data were fit to the standard charge balance equation for *n*-type conduction, which assumes that the activation is from donor levels,[18]

$$n + K = \sum_i \frac{N_{d_i}}{1 + (ng_i/N_C)e^{E_{a_i}/kT}}, \tag{2}$$

where N_{d_i}, E_{a_i} and g_i are the concentration, activation energy, and degeneracy, respectively, of the ith donor level, K is the total acceptor concentration minus the total shallow donor

Downloaded 14 Aug 2007 to 132.250.134.160. Redistribution subject to AIP license or copyright, see http://jap.aip.org/jap/copyright.jsp

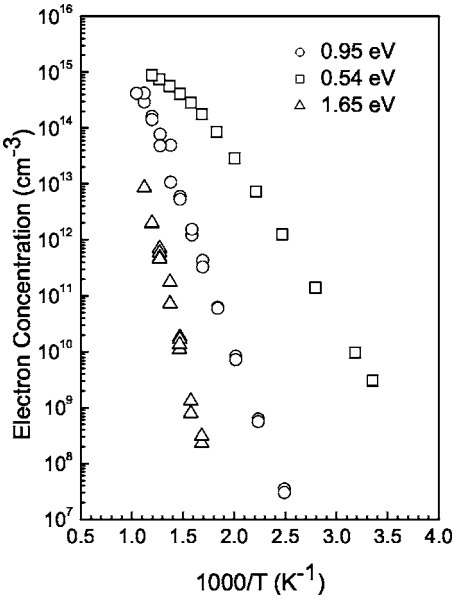

FIG. 1. Carrier concentration vs inverse temperature for three HPSI 4*H*-SiC samples indicating the variation in E_a's observed in this study.

concentration, and $N_C=2M_C(2\pi m^* kT/h^2)^{3/2}$ is the density of states in the conduction band, where M_C is the number of conduction band minimum, taken to be 3, and $m^*=0.390$ is the electron effective mass. g is the degeneracy factor for the level and was taken to be 2 for all donors and donorlike defects. M_C and m^* were taken from the work of Persson and Lindefelt.[19]

In addition, we consider the possibility that the free electrons we measure are due to neutralization of compensated deep acceptors in the upper half of the band gap rather than ionization of deep donors. Look and Sizelove[20] give a charge balance equation similar to Eq. (2) above for the case of deep acceptors in the upper half of the band gap,

$$n + K + \sum_i \frac{N_{da_i}}{1 + (N_C/ng_i)e^{-E_{a_i}/kT}} = 0, \tag{3}$$

where K here is the total concentration of the shallow, fully compensated, acceptors minus the concentration of all donors. The other terms have the same meaning as in Eq. (2).

However, as Look and Sizelove[20] demonstrate, the two equations give identical deep level concentrations and activation energies. The only difference between the two is the value of the concentration of compensating centers. If the standard equation [Eq. (2)] was used for the case of deep acceptors, the fitted value of K would actually be the true K minus the deep level concentration and thus a smaller number than the real K. Therefore, to distinguish deep acceptors from deep donors other information must be available and we use SIMS measurements of the nitrogen and boron concentrations to help resolve the issue.

RESULTS

Figure 1 shows the electron concentration versus inverse temperature results for three HPSI samples representing the range of activation energies observed in this study. A total of 16 samples were investigated for this study. When the scatter in the data was low, the activation energies E_a were determined from fits of the carrier concentration versus inverse temperature data to either the simple exponential behavior of Eq. (1) or the charge balance equation [Eqs. (2) and (3)]. Otherwise E_a was determined by fitting the resistivity versus inverse temperature data to Eq. (1). Figure 2 shows the resistivity versus inverse temperature data for a sample with a resistivity E_a of 1.65 eV along with that of a sample with a much lower resistivity. The lower resistivity data in Fig. 2 is from a developmental sample (B) with $E_a=E_C-0.55$ eV from carrier concentration fitting which is semi-insulating at room temperature but clearly fails the commonly used 1×10^5 Ω cm definition at elevated temperatures.

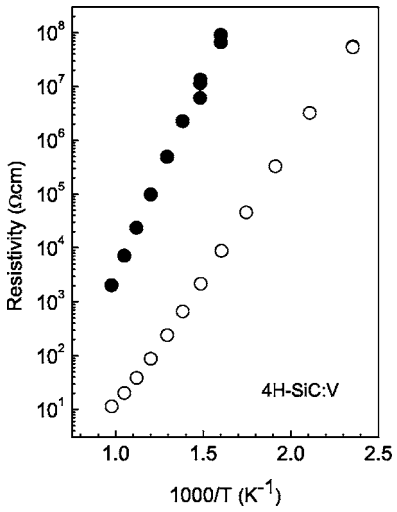

FIG. 2. Resistivity vs inverse temperature for samples B and H.

The E_a results for all the samples studied are presented graphically in Fig. 3. All activation energies obtained from carrier concentration data are measured from the bottom of the conduction band since all samples with measurable Hall coefficients were n type. There are three samples with E_a's around 0.55 eV, but the demarcations between other deep levels are difficult to distinguish in this data set. The 1.1 eV level reported by the authors previously[3] is hardly distinguishable from two samples with E_a's around 0.95 eV, and it is not clear if there are one or two midgap levels. It should also be noted that the level at $E_C-0.55$ eV has not been reported by other researchers. Son *et al.*[8] reported a set of

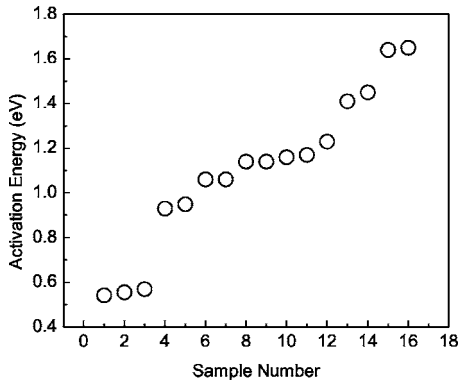

FIG. 3. Activation energies for all of the samples in this study showing a variation from 0.55 to 1.65 eV.

Downloaded 14 Aug 2007 to 132.250.134.160. Redistribution subject to AIP license or copyright, see http://jap.aip.org/jap/copyright.jsp

TABLE II. Carrier concentration fitting results for HPSI 4*H*-SiC samples. N_{DL_i}=concentration of *i*th deep level, E_{DL_i}=activation energy of *i*th deep level measured from the top of the conduction band edge, $(N_{SA}-N_{SD})_d$ =shallow acceptor concentration minus shallow donor concentration determined from Eq. (2) assuming that deep levels are donors, and $(N_{SA}-N_{SD})_a$=shallow acceptor concentration minus shallow donor concentration determined from Eq. (3) assuming that deep levels are acceptors.

Sample	N_{DL_1} (cm^{-3})	E_{DL_1} (eV)	N_{DL_2} (cm^{-3})	E_{DL_2} (eV)	$(N_{SA}-N_{SD})_d$ (cm^{-3})	$(N_{SA}-N_{SD})_a$ (cm^{-3})
A	1.0×10^{15}	0.54	8.8×10^{14}	0.72	5.0×10^{14}	-1.4×10^{15}
B	3.8×10^{15}	0.55	···	···	3.7×10^{14}	-3.5×10^{15}
C	1.1×10^{15}	0.56	1.4×10^{15}	0.80	4.3×10^{14}	-2.0×10^{15}
F	2.6×10^{15}	0.93	···	···	3.1×10^{14}	-2.3×10^{15}

samples with E_a's, determined from resistivity measurements, in the range of 0.6–0.7 eV. The resistivity versus inverse temperature for sample B with E_a=0.55 eV is shown in Fig. 2. We attempted to use Eq. (1) to determine a resistivity activation energy for this sample using smaller, straighter, temperature segments below the saturation region at high temperature, where the temperature dependence of the mobility starts to play a large role in the temperature dependence of the resistivity but in every case the activation energy determined in this manner was always less than 0.55 eV.

The carrier concentration data for four samples with the lowest E_a's in Fig. 3 were fit to both Eqs. (2) and (3). These samples all showed evidence of the onset of saturation of the carrier concentration at high temperatures which the permitted use of the charge balance equations to determine deep level concentrations and the concentrations of the compensating shallow donors and acceptors. The results are shown in Table II. The $\log(n)$ vs $1/T$ plots for all the other samples in this study were straight lines with no evidence of saturation. The lack of saturation permits the determination of an activation energy by fits to Eq. (2) or (3) but not concentrations because the fitted concentration values are not unique. As expected, the fits for the four samples with the different equations gave nearly identical results, except for the compensation values. The results are presented in Table II. The deep level concentrations and activation energies were the same for the two fits and so are only listed once. The two level fits for samples A and C were significantly better than the one level fits, indicating the presence of another level further from the conduction band edge. The one and two level fits for sample A are shown as dashed and solid lines, respectively, in Fig. 4 along with the data. It should be noted that the second level would not be detected if it is the opposite type from the first level, in such a situation it would be included in the compensation and not as a separate level. We note that Müller *et al.*[21] reported a level at 0.8 eV, similar to the second level in sample C.

SIMS measurements were made on three samples with different activation energies. Samples were cut from the same wafers as the van der Pauw samples and measurements were made in this laboratory and at external laboratories. Boron and nitrogen, both in the 10^{15} cm^{-3} range, were the dominant impurities. All other impurities were either at or below the detection limit, or in the low 10^{14} cm^{-3} range, and were thus not considered important. The results of SIMS measurements made by Cree on similar material can be found in Ref. 2 Our boron and nitrogen results are presented in Fig. 5 with the uncertainty, which includes the overall precision of the measurement and the uncertainty on the relative sensitivity factor, for samples B (0.55 eV), E (1.65 eV), and F (0.93 eV). In addition we have included nitrogen concentrations determined from photoluminescence measurements[22] which are in general agreement with the SIMS results. While the concentrations of both boron and nitrogen are clearly in the mid-10^{15}-cm^{-3} range, and that of the nitrogen concentration exceeds the boron concentration, the differences between nitrogen and boron concentrations

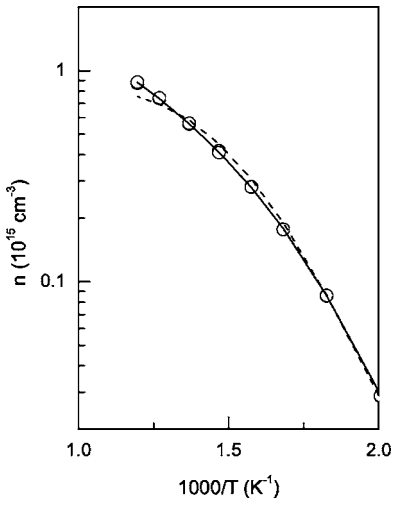

FIG. 4. One and two level fits to Eq. (3) for sample A. (Circles) data, (dashed line) one level fit, and (solid line) two level fit.

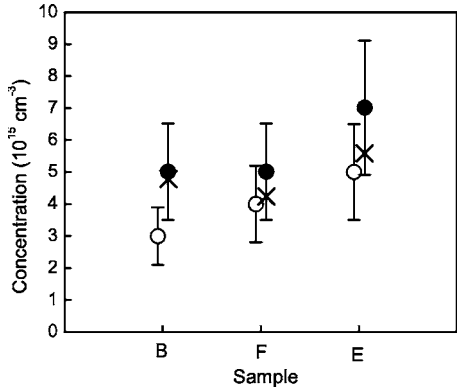

FIG. 5. Nitrogen and boron concentrations for samples. (Solid circles) SIMS nitrogen results, (crosses) PL nitrogen results, and (open circles) SIMS boron results.

Downloaded 14 Aug 2007 to 132.250.134.160. Redistribution subject to AIP license or copyright, see http://jap.aip.org/jap/copyright.jsp

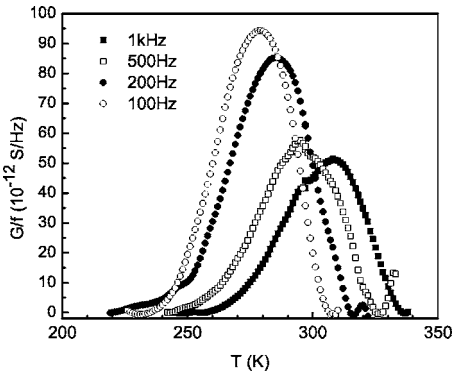

FIG. 6. Thermal admittance spectroscopy results for sample A.

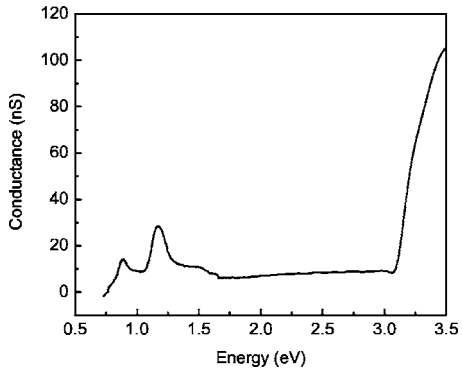

FIG. 8. Optical admittance spectroscopy results for sample B in the range from 0.8 to 3.2 eV.

are on the order of the experimental uncertainty. Within the limitations of the uncertainty, the SIMS results are in general agreement with the N_{SA}-N_{SD} values obtained from the deep acceptor fits model in Table II for the 0.55 eV sample.

TAS and OAS measurements were made on samples A and B to confirm the presence of the 0.55 eV level and to determine if other deep levels are present. Figure 6 shows a TAS spectra for a sample from wafer A. Fits to the Arrhenius plot of the peak frequency to inverse temperature gave an activation energy of 0.512 eV for sample A and 0.551 eV for sample B, in very close agreement with the TDH results. OAS measurements were made on the same samples and results for sample A are shown in Fig. 7. Peak fitting of the spectra in the figure indicated four peaks, two strong peaks at 0.55 and 0.64 eV that merge to make the dominant spectral feature around 0.6 eV and two on the high energy shoulder at 0.73 and 0.93 eV. These could be hexagonal and cubic lattice site levels for the 0.55 eV level and the deeper level at 0.72 seen in carrier concentration data. However, four peaks, at 0.56, 0.64, 0.76, and 0.83 eV, were also observed in sample B, in which a second deep level could not be extracted from carrier concentration fits. Intrinsic levels at energies above 0.9 eV in HPSI material have proven extremely difficult to detect with OAS, and most of the samples in this study showed no measurable response in the region from 1.0 to about 2.5 eV. This effect is not understood but it could be due to low optical cross sections of the deep levels or short carrier lifetimes. However, as seen in Fig. 8, two peaks were observed at 0.88 and 1.2 eV in the sample from wafer B.

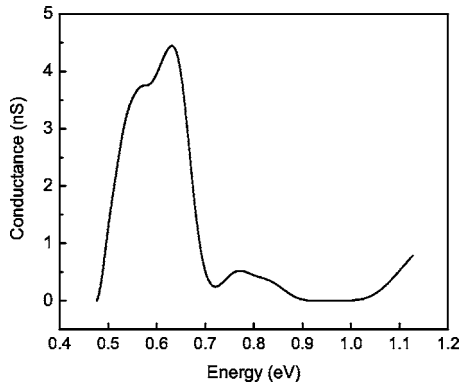

FIG. 7. Optical admittance spectroscopy results in the range from 0.5 to 1.0 eV.

These OAS results suggest that at least some of the samples in this study have deep levels present at larger energies than those determined from the Hall effect experiments and that the Fermi level location is determined by relative concentrations of all of the deep levels and the compensating shallow levels. This is in contrast to the results on undoped semi-insulating 6*H*-SiC from another source reported earlier by this group,[23] where the evidence suggested that only one deep level played an important role in the compensation mechanism.

To investigate the thermal stability of the deep levels several samples with different activation energies were annealed at 1600 °C for 30 min in argon. Figure 9 shows the resistivity of samples I (1.41 eV) and Q (1.14 eV) before and after the 1600 °C annealing. The 1.41 eV sample showed little to no variation in resistivity while the resistivity for the 1.14 eV sample decreased slightly. The activation energies did not change. Figure 10 shows the carrier concentration for sample B and another, adjacent sample from the same wafer after 1600 °C annealing. The one level fits to Eqs. (2) and (3) for the annealed sample gave a deep level concentration of 2.2×10^{15} cm^{-3} and an activation energy of 0.53 eV, compared to 3.8×10^{15} cm^{-3} and 0.554 eV for the unannealed sample. Other levels could not be detected. Fig-

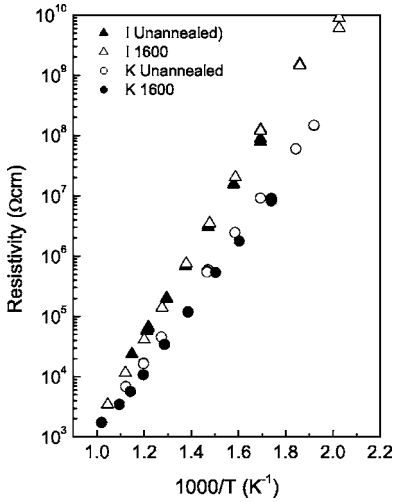

FIG. 9. Resistivity vs inverse temperature before (open symbols) and after (solid symbols) annealing at 1600 °C. (△) sample I (E_a=1.4 eV) and (○) sample K with (E_a=1.2 eV).

Downloaded 14 Aug 2007 to 132.250.134.160. Redistribution subject to AIP license or copyright, see http://jap.aip.org/jap/copyright.jsp

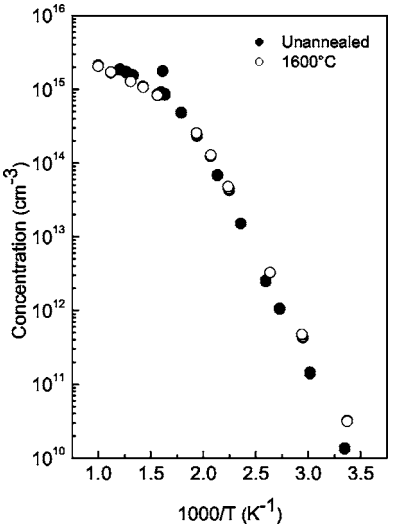

FIG. 10. Carrier concentration vs inverse temperature for unannealed 0.55 eV sample B (solid circles) and a sample from the same wafer annealed at 1600 °C (open circles).

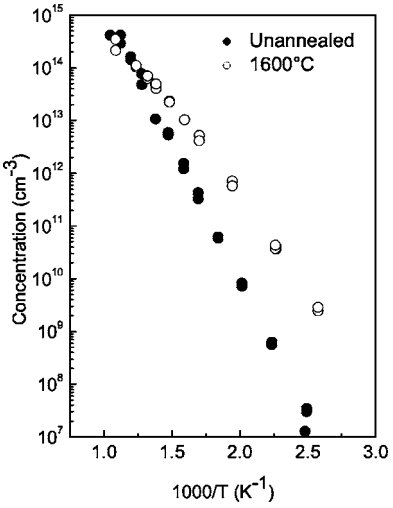

FIG. 11. Carrier concentration vs inverse temperature for sample D (0.95 eV) before (open circles) and after (solid circles) annealing at 1600 °C.

ure 11 shows the annealing results for sample D, which had an activation energy of 0.95 eV before annealing. The best fit after annealing was a two level fit to Eq. (3) which gave 2.3×10^{15} cm^{-3} and 0.45 eV for the concentration and energy of the first level and 8.9×10^{14} cm^{-3} and 0.97 eV for the second level, which is most likely the same level as before annealing. It should be noted that the mobilities after annealing were unchanged from the unannealed values.

DISCUSSION

One of the unresolved questions in HPSI SiC is whether the intrinsic deep levels are donors or acceptors. The *n*-type conduction observed here confirms that these deep levels are all in the upper half of the band gap. While not conclusive, the SIMS results in combination with fits to the two charge balance equations suggest that at least the levels near 0.55 and 0.95 eV are acceptorlike. All fits assuming that the deep levels are donorlike gave N_{SA}-N_{SD} in the low to mid-10^{14}-cm^{-3} range, but the SIMS results reported here and elsewhere on similar material[2] indicate that the boron and nitrogen concentrations are in the mid-10^{15}-cm^{-3} range. The fits assuming that the levels are deep acceptors, however, give values that are consistent with the SIMS results. It is therefore reasonable to assume that at least the 0.55 and the 0.93 eV levels are acceptorlike.

The concentrations for sample C in Table II are worth special consideration. As can be seen, the sum of the concentrations of the two deep levels is actually less than the N_{SA}-N_{SD} value. This means that neither deep level acting alone has sufficient concentration to compensate the shallow level impurities but that both together can. It should be noted here that, unlike in the deep donor case, the deep acceptor level (further from the conduction band) is fully compensated. Further, the concentrations of all the 0.55 and 0.93 eV deep levels determined by charge balance equation fitting are individually below the concentrations of nitrogen and boron determined by SIMS and almost always below the difference in concentrations of these impurities. Also, as can be seen in Fig. 1, the electron concentrations for none of the deep levels (1.1, 1.4 eV, etc.) ever exceed low 10^{14} cm^{-3} at the highest measurement temperatures, which suggests that their deep level concentrations are on the same order as those for the shallower levels. Further support for the presence of multiple deep levels in this material comes from the admittance spectroscopy results but concentrations were not determined from these techniques. All these indicate that the deep levels in HPSI 4*H*-SiC studied here by TDH are individually unable to compensate the shallow impurities and produce semi-insulating material. The concentrations of intrinsic defects observed by EPR measurements of the material in this study[24] are also too low to produce semi-insulating material by themselves. Thus, multiple deep levels whose total concentration exceeds N_{SA}-N_{SD} are required. We suggest that several deep levels are present in varying concentrations in all of the samples studied here and that the Fermi level position is determined primarily by variations in the shallow impurity concentrations, with different deep levels pinning the Fermi level as the difference in shallow acceptors and donors varies. However, the SIMS results suggest that all of the deep levels are never present in any one sample. When the deep levels are acceptorlike in the upper half of the band gap it is the compensated centers that contribute to the conduction and pin the Fermi level, not the uncompensated centers as with donorlike defects. The electrons from the shallow donors will compensate the lowest acceptors (closest to the valence band edge) first, starting with the acceptor impurities such as boron and aluminum and moving upwards through the 1.6 eV level to the 0.55 eV level. The Fermi level will be pinned at the highest acceptor level to be partially compensated. Totally uncompensated levels closer to the conduction band edge will not be detected because there are no electrons on them available for excitation to the conduction band. This means that there must be enough nitrogen to compensate the shallow acceptors and all of the deep acceptor levels below the Fermi level. Therefore, if levels at 1.6, 1.1, and 0.93 eV were all present in the 0.55 eV samples at concentrations in the low 10^{15} cm^{-3} range, the nitrogen

Downloaded 14 Aug 2007 to 132.250.134.160. Redistribution subject to AIP license or copyright, see http://jap.aip.org/jap/copyright.jsp

concentration would have to be significantly higher than the boron concentration but significantly lower than that in the 1.6 eV sample, and this is not observed. In fact, the contamination in the 1.6 eV sample is higher than in the other samples studied by SIMS. The lack of saturation in the TDH data for the samples with E_a between 1.6 and 1.4 eV prevents reliable analysis of the compensation and it is possible that there are different deep levels in this range, one or more of which could be donorlike but we have not observed any specific evidence for donorlike intrinsic defects.

The annealing studies reported here indicate that most of the deep levels in this material are relatively stable at 1600 °C, which should be expected since the crystals were grown at much higher temperatures. The 0.93 eV sample is the only exception and its annealing behavior supports the hypothesis that the 0.55 eV level is present in most samples but uncompensated in samples with a deep Fermi level. Reduction of the 0.93 eV level by annealing would move the Fermi level to the next higher acceptorlike level, which is what appears to be happening, although the fits are not as good as those for the unannealed 0.55 eV samples and the energy is not as close to 0.55 eV as could be hoped for. All of these results demonstrate that compensation in the HPSI samples studied here is complex and involves many deep levels.

The level near 0.55 eV has not, to our knowledge, been reported previously. As mentioned above, Son *et al.*[8] report a level in the 0.6–0.7 eV range. Even though this is too high to be the level observed here, since we do not observe E_a's in this range, we must assume that their 0.6–0.7 eV level is the same defect as the 0.55 eV level reported here. It is possible that they are observing the deeper of the two OAS levels (0.64 eV) reported here that we associate with the 0.55 eV level, but it is not clear why they would not also observe the shallower level. We also note that no other experiments have seen the two OAS levels together at the energies reported here.

CONCLUSIONS

Deep levels in HPSI 4*H*-SiC have been studied with TDH, TAS, OAS, and SIMS. Activation energies between $E_C-0.55$ and $E_C-1.6$ eV were detected by TDH. The presence of levels between 0.55 and 1.2 eV has been confirmed by TAS and OAS. Studies of compensation in samples with the Fermi level pinned closer to the conduction band than 1.0 eV indicate that the deep levels are acceptorlike. The results show that the concentrations of individual deep level defects are insufficient to compensate residual nitrogen and boron impurities. A model is proposed in which multiple deep levels act together to compensate the shallow impurities and produce semi-insulating material. All but one of the deep levels observed were found to be thermally stable at 1600 °C. A previously unreported level at $E_C-0.55$ eV is reported. Its nature could not be determined.

ACKNOWLEDGMENTS

The authors wish to thank Patrick Johnson for valuable technical assistance and Dr. D. Dorsey of AFRL for supporting this project. This work was partially supported by DARPA Wide Bandgap Semiconductor Technology Initiative which also provided samples. Some of the samples were provided by the U.S. Air Force Title III office (Robert Drerup).

[1] W. C. Mitchel *et al.*, Mater. Sci. Forum **338–342**, 21 (2000).
[2] J. R. Jenny *et al.*, Mater. Sci. Forum **457–460**, 35 (2004).
[3] W. C. Mitchel, W. D. Mitchell, M. E. Zvanut, and G. Landis, Solid-State Electron. **48**, 1693 (2004).
[4] V. Konovalov, M. E. Zvanut, V. F. Tsvetkov, J. R. Jenny, St. G. Müller, and H. McD. Hobgood, Physica B **308–310**, 671 (2001).
[5] E. N. Kalabukhova, S. N. Lukin, A. Saxler, W. C. Mitchel, S. R. Smith, and J. S. Solomon, Phys. Rev. B **64**, 235202 (2001).
[6] W. E. Carlos, E. R. Glaser, and B. V. Shanabrook, Physica B **340–342**, 151 (2003).
[7] N. T. Son, B. Magnusson, Z. Zolnai, A. Ellison, and E. Janzén, Mater. Sci. Forum **457–460**, 437 (2004).
[8] N. T. Son, P. Carlsson, B. Magnusson, and E. Janzén, Mater. Res. Soc. Symp. Proc. **911**, 201 (2006).
[9] M. E. Zvanut, W. Lee, H. Wang, W. C. Mitchel, and W. D. Mitchell, Mater. Sci. Forum **527–529**, 517 (2006).
[10] W. E. Carlos, E. R. Glaser, and B. V. Shanabrook, Physica B **340–342**, 151 (2003).
[11] T. Dalibor, G. Pensl, H. Matsunami, T. Kimoto, W. J. Choyke, A. Schöner, and N. Nordell, Phys. Status Solidi A **162**, 199 (1997).
[12] A. A. Lebedev, Semiconductors **33**, 107 (1999).
[13] C. Hemmingsson, N. T. Son, O. Kordina, J. P. Bergman, and E. Janzén, J. Appl. Phys. **81**, 6155 (1997).
[14] L. Storasta, J. P. Bergman, E. Janzén, and A. Henry, J. Appl. Phys. **96**, 4909 (2004).
[15] J. Zhang, L. Storasta, J. P. Bergman, N. T. Son, and E. Janzén, J. Appl. Phys. **93**, 4708 (2003).
[16] K. Danno, T. Kimoto and H. Matsunami, Appl. Phys. Lett. **86**, 122104 (2005).
[17] T. Negoro, T. Kimoto, and H. Matsunami, Appl. Phys. Lett. **85**, 1716 (2004).
[18] See, for example, D. C. Look, in Semiconductors and Semimetals Vol. 19, edited by R. K. Willardson and A. C. Beer (Academic, New York, 1983), p. 75.
[19] C. Persson and U. Lindefelt, J. Appl. Phys. **82**, 5496 (1997).
[20] D. C. Look and J. R. Sizelove, J. Appl. Phys. **61**, 1650 (1987); D. C. Look, *ibid.* **62**, 3998 (1987).
[21] St. G. Müller *et al.*, Eur. Phys. J.: Appl. Phys. **27**, 29 (2004).
[22] E. R. Glaser, B. V. Shanabrook, and W. E. Carlos, Appl. Phys. Lett. **86**, 052109 (2005).
[23] W. C. Mitchel *et al.*, J. Appl. Phys. **100**, 043706 (2006).
[24] W. C. Mitchel, W. D. Mitchell, H. E. Smith, W. E. Carlos, and E. R. Glaser, Mater. Res. Soc. Symp. Proc. **911**, B06-02 (2006).

Downloaded 14 Aug 2007 to 132.250.134.160. Redistribution subject to AIP license or copyright, see http://jap.aip.org/jap/copyright.jsp